ISSN 1392-2114 ULTRAGARSAS, Nr.2(35). 2000.

The ultrasonic field in lossy media: some simulation and experimental results

R. Jurkonis, A. Lukoševičius

Ultrasound Biomedical Engineering Lab., Kaunas University of Technology.

Introduction

The subject of the paper is simulation and measurements of an ultrasonic field in an isotropic homogeneous medium with attenuation. The complex problem of simultaneous influence of wave diffraction, attenuation, and velocity dispersion occurs. Only few publications can be mentioned on this subject. For example in [1] is presented an investigation of the complex problem of ultrasound field distribution in lossy media, taking into account both the radiation of the ultrasonic signal by finite aperture and attenuation in media having velocity dispersion. The solution in frequency domain is presented here. The method is based on the use of complex wave-number $k(\omega)$, therefore analysis in space-spectra domain is called a "k-space" calculation of ultrasonic field distributions. In [1], the main conclusion states the following: for typical linear arrays and typical biological media, the image (B-scan) modification due to medium absorption is caused mainly by the magnitude modifications of different frequency components, but not by pulse modification due to phase velocity differences of those frequency components.

Another calculation method for ultrasonic field in attenuating medium is presented in [2]. Therein, the radiation of aperture and field distribution is analysed on the basis of three-dimensional impulse response of aperture. According to Huygen's principle, the spherical waves are emitted by elementary sources on the aperture. The attenuating medium modifies the propagation of spherical waves, which continuously depend on the distance from the aperture. The calculation of field is done in far-field (Fraunhofer) region, which does not reveal the main point of continuos modification of wave propagation.

The mathematical expressions necessary for the simulation of transient or stationary ultrasonic fields in attenuating media has been summarised in [3], the minimum-phase filter approach was developed in [4]. Natural wave propagation in terms of linear acoustics is analysed. One of the basic assumptions is that speed of sound does not depend on the acoustic path length and remains constant c_0 within all the media under investigation. The medium is described as homogeneously attenuating medium, where attenuation is caused by ultrasonic energy absorption only.

In the present paper the one-dimensional problem of ultrasound attenuation and velocity dispersion is investigated theoretically and experimentally as a first step. Two models were applied, both having mutually related attenuation and velocity dispersion: 1) time-causal model; 2) minimum-phase filter model. Then the three-dimensional situation was simulated; in this case the interference of waves in lossy media was concerned. Results are presented showing the simultaneous influence of attenuation and diffraction in the three-dimensional approach on the wave-front and zero-crossings of space-distributed pulse signal. The comparison of simulations and experimental results are shown. Minimum-phase and time-causal models were applied in the calculations.

The main goal of the paper is to simulate wave attenuation and velocity dispersion in space, taking into account the causality principle. Some simulation results obtained were compared with experimental measurements and the findings discussed. Must be pointed that present paper is the continuation of earlier one [3] which could help to clarify results presented herein.

Attenuation model

Attenuation of ultrasonic wave can be simply described by the frequency function [5,8]:

$$\alpha(f) = \alpha_0 \cdot f^{\,y}, \qquad (1)$$

here: α_0 is an attenuation coefficient having the units of dB/(cm MHz^y), f – is the frequency. The product of $\alpha(f)$ and R determines the loss of amplitude for a particular frequency wave passing the acoustic path of length R.

According to theory of linear systems, a layer of media of thickness R can by described as an acoustic system, having frequency response [5]:

$$H(\omega) = e^{-\alpha(\omega)R} \cdot e^{-j\beta(\omega)R}, \qquad (2)$$

here: $e^{-\alpha(\omega)R}$ - is the amplitude frequency response, $\beta(\omega)R$ - is the phase frequency response. That means that the travelling path length R and attenuation rate $\alpha(f)$ here are mathematically inseparable.

Therefore, to describe adequately propagation of the wave in the medium, is necessary to know the loss factor of wave amplitude and wave propagation velocity. The attenuation and velocity are the related medium features if on such medium based acoustic system is assumed to be linear and causal [7,8]. On the authors opinion at present the best performing approaches establishing such relation and suitable to incorporate into the ultrasonic field model are applied and discussed.

Spectrum domain simulation

It is assumed that at each elementary time instant, a set of spectrum components is emitted from the aperture. Each set of spectrum components has a particular set of attenuation and propagation velocities. "Split spectrum" formulation used in order to simulate the plane wave propagation of broadband ultrasound pulse in a lossy medium is proposed in [5] taking in account attenuation described by formula (2). Using a bank of Gaussian filters, the broadband pulse is firstly decomposed into narrowband components. The simulation of effects of the attenuation

and velocity dispersion is then applied on each component separately. The resulting waveform is constructed again according to principle of superposition. If the bandwidth of each component is narrow enough, only the centre frequency of the component can be evaluated, resulting in a magnitude reduction, a constant phase angle lag, and a relative time delay.

The presented method for the output signal simulation does not invoke the impulse response of the system and does not need the assumption about the attenuation dependency in a certain frequency range. While implementing the method, the attenuation is measured only over the frequency range of input signal, and the dispersion is derived from the measured attenuation over the same frequency range [7].

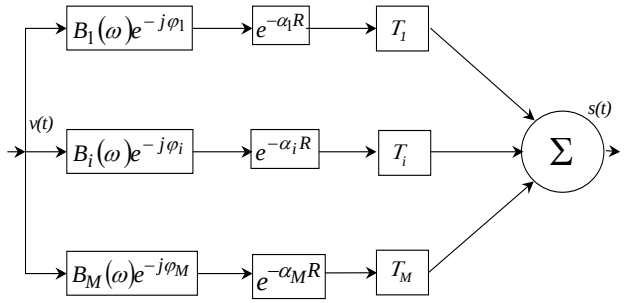

Fig.1. **The procedures used to simulate the output pulse *s(t)*. The incident pulse *v(t)* firstly passes through bandpass filters having a Gaussian magnitude function $B_i(\omega)$ and a constant phase angle $-\varphi_i$. Each component signal is then scaled down by an exponential factor $exp(-\alpha_i R)$ and relatively delayed by T_i. All components are then added together to produce the modified pulse *s(t)* at the output**.

The model originating from time-causal theory and enabling calculation of the dispersion from the local attenuation was proposed in [6] and is referred to as the time-causal model. The time-causal model enables one to calculate the phase velocity from the attenuation values near a reference frequency ω_0. This time-causal model adapted for the split spectrum approach consists of two following basic expressions (3) and (4). For the case $y>1$, the relative time delay T_{ni}:

$$T_{ni} = R_n\left\{\frac{1}{c_0} + \alpha_0\left(y\omega_i^{y-1} - \omega_0^{y-1}\right)\tan\left(\frac{y\pi}{2}\right)\right\}, \qquad (3)$$

and phase angle φ_{ni} :

$$\varphi_{ni} = -(y-1)\omega_i^{y}\alpha_0 R_n \tan\left(\frac{y\pi}{2}\right), \qquad (4)$$

here, c_0 is the phase velocity at a reference frequency ω_0, i - the index of the spectrum component, $R_n = z + nc_0\tau$ - the current path of signal propagation in terms of medium layer thickness [3], z – is the distance from aperture, n - is the an index of the discrete time instant.

Using expressions (3) and (4) and procedures drawn in Fig.1 *i-th* narrowband component is described as follows:

$$s_{ni}(t, R_n) = FFT^{-1}\left\{B_i(\omega)\cdot e^{-\alpha_i R_n - j(\varphi_{ni}+\omega T_{ni})}\right\}, \qquad (5)$$

here: i is an index of the same meaning as in (3) and (4),

In order to simulate the ultrasonic field the calculation of aperture impulse response is needed. In [3] the expression for aperture impulse response in attenuating medium is given:

$$h_\alpha(t, x, y, z) = \sum_{n=0}^{N-1}\left\{g_{\alpha_n}(t - n\tau, R_n)\cdot h(n\tau, x, y, z)\right\}, \qquad (6)$$

here: $\sum\{*\}$ - is the sum of N sequences element-by-element, $g_{\alpha_n}(t, R_n)$ - is the impulse response of isotropic homogeneous medium layer between *n-th* equidistant line on the emitting aperture and the point in space under investigation, $h(t,x,y,z)$ – aperture spatial impulse response in ideal medium sampled with τ time interval.

In the case of time-causal model performed using spectrum decomposition, the aperture response $h(t,x,y,z)$ defines the amplitude and the time interval within which narrowband contributions caused by particular aperture geometry are possible. So, the transient reaction for acoustic pressure in a space point under investigation is:

$$p_\alpha(t,x,y,z) = \frac{\partial}{\partial t}\left\{\sum_{n=0}^{N-1}\left[\sum_{i=1}^{M} s_{ni}(t - n\tau, R_n)\cdot h(n\tau, x, y, z)\right]\right\}, \qquad (7)$$

here M – is the number of narrowband components. Because $h(t,x,y,z)$ is calculated as the impulse response for a velocity potential and $s_{ni}(t,R_n)$ is the attenuated and dispersed waveform of vibrations velocity $v(t)$ on the aperture, the convolution result has the meaning of velocity potential. Therefore to obtain acoustic pressure the time derivative is taken.

Simulation of impulse response

The approach to describe an unknown system by using impulse response is well known in electrical engineering theory and practice. This is the way to describe a system just functionally, without an explanation of the physical effects present.

Unlike in electrical network applications of the Kramers-Kronig relations, acoustics pose unique problem [5]. In acoustics, the propagation problems may occur in the stage of assumptions. For example, assuming a power-law dependence of attenuation on frequency in (2). The Paley-Wiener theorem states that for a transfer function of the form (2) the logarithm of the amplitude response must meet the requirement [9]:

$$\int_{-\infty}^{\infty}\frac{\left|\ln\left(e^{-\alpha(\omega)R}\right)\right|}{1+\omega^2}d\omega = \int_{-\infty}^{\infty}\frac{\left|-\alpha(\omega)R\right|}{1+\omega^2}d\omega < \infty, \qquad (8)$$

and therefore $\alpha(\omega)$ must be square-integrable in order for causality to hold. These requirements restrict values of y to be less than one.

But in [7] Ping He mentions that in cases $y \geq 1$ (the usual case for biological tissue for example) the difference of results obtained in the time-causal model and in the minimum-phase model depends on the cut-off frequency in integral (8). This approach leads to minimum-phase model for a layer of tissue. For a minimum-phase system, frequency responses of attenuation (or amplitude) and phase are related by a Hilbert transform. Because of this property, the complex transfer function $H(\omega)$ and the corresponding impulse response $g_\alpha(t)$ of the layer can be obtained from the known attenuation $\alpha(f)$ of the medium.

So, an alternative to time-causal model, in the minimum-phase filter approach the discrete Hilbert transform was applied to calculate velocity dispersion [3]:

$$g_{\alpha_n}(t,R_n) = FFT^{-1}\left\{e^{[-\alpha_n(f,R_n)-j\beta_n(f,R_n)]}\right\}, \quad (9)$$

$$\alpha_n(f,R_n) = \alpha_0 \cdot f^{\,y} \cdot R_n, \quad (10)$$

$$\beta_n(f,R_n) = HT\{\alpha_n(f,R_n)\}, \quad (11)$$

here: $g_{\alpha_n}(t,R_n)$ - the impulse response n-th layer, $HT\{*\}$- denotes operation of the discrete Hilbert transform, $\beta_n(f,R_n)$ – dispersive part of phase frequency response, $R_n = z + nc_0\tau$ - the current path of signal propagation in terms of medium layer thickness [3].

When such an approach is applied for a simulation of a tissue layer, one is facing two problems here [5]. First of all, the Hilbert transform relation between attenuation and dispersion are defined in such a way that, in order to obtain the value of one of them at any single frequency, it is necessary to know the values of the other one at all frequencies. Therefore, the problem is to validate the assumption that the values of $\alpha(\omega)$ at all frequencies can be correctly extrapolated from the measured values. Secondly, the problem of keeping the causality of the model which is incorporated in (8). Kuc [4] circumvented the problem associated with the Paley-Wiener condition, by implementing the minimum-phase model in the discrete-frequency domain. In such a case, the folding frequency (*1/2* of sampling frequency) becomes the natural high-frequency limit. Therefore the discrete Hilbert transform is employed in the presented simulations.

The field simulation in the lossy media can be done by the method presented and explained in [2,3]. This method is flexible in terms of description of media features, because of the application of the system transfer function which consists of amplitude and phase frequency responses only. All newly developed expressions for ultrasound wave attenuation and related velocity dispersion can be easily incorporated into the proposed model of the field.

Experimental test

The purpose of the experimental investigations was to verify how accurately the features of a broadband ultrasonic pulse could be simulated using the proposed models, including verification of both the attenuation and the velocity dispersion effects in the lossy media. Experiments were performed in the lossless media (distilled water) and in highly absorptive media – castor oil. An ultrasonic pulse with 14 MHz central frequency of spectrum was used. An originally designed keratometry system was used including a special broadband ultrasonic transducer and transmit-receive electronics (Fig.2). The ultrasonic signal was investigated at first keeping the one-dimensional assumption. The transducer had the following construction: disk piezoceramic element 2,4 mm in diameter, with a focusing plexiglass concave lens on it, and a water filled acoustic waveguide 15 mm in length. The transducer was designed for the focus distance to be equal to 15 mm,- at the end of a water-filled waveguide. The radiator of such a configuration is considered as the source of plane ultrasonic waves. The reflection at interface water - plexiglass and castor oil – plexiglass was assumed to be perfect without any influence on the spectra of the reflected pulse. The perpendicular acoustic path towards the plexiglass plane was aligned carefully seeking maximum amplitude of multiple reflections of the pulse.

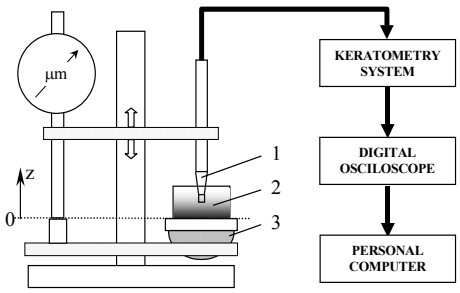

Fig.2. **The set-up of the system for experimental investigation of propagation of broadband ultrasonic pulses in lossy media: 1 – ultrasonic pulse transducer of *14* MHz central frequency with acoustical waveguide; 2 - small bath with plexiglas bottom; 3 – segment of ball for adjustment of the reflecting plane perpendicularly to the acoustic beam.**

A micro-screw mechanism and micrometer were used for precise changes in the length of the acoustic path in the media layer strictly along the axis *z*. The distance from the top of transducer to the reflector was changed in the range of 0,30…3,00 mm in steps of 0,10 mm. The reflected pulse signal was digitised using TEKTRONIX TDS 220 digital oscilloscope with, a sample rate of 1 GS/s and a resolution of 8 bit. The frequency bandwidth of the oscilloscope for analogue signal is 100 MHz.

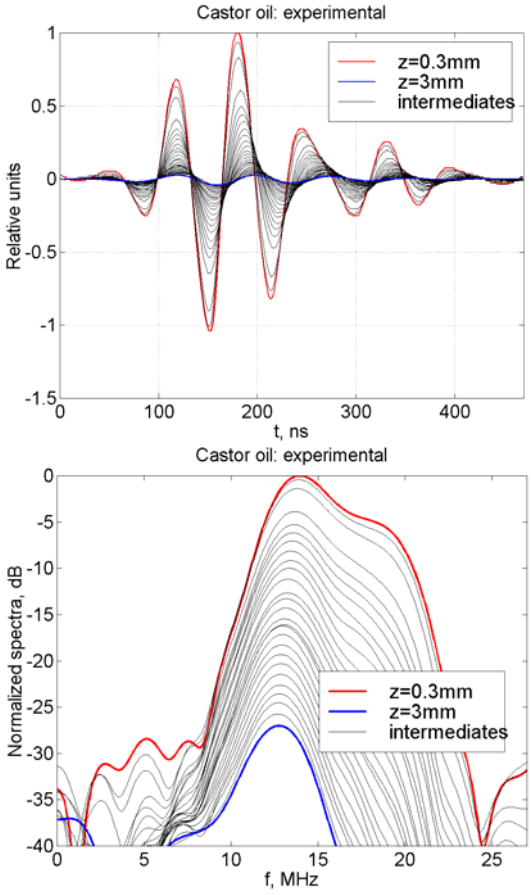

Fig.3. **Experimental data: set of echo-pulses acquired through castor oil and the corresponding set of spectra**.

128 waveforms were averaged during an acquisition. After 28 (range of 0,30…3,00 mm) echo-pulses were acquired working through distilled water, the bath was filled with castor oil (Oleum ricini; AB Herbapol Kleka, Nowe Miasto nad Warta, Poland) to repeat the test in the same conditions. The normalised attenuation coefficient for castor oil was α_0=0,7 dB/(cm MHz$^{1.67}$) [7], and for water α_0=0,0022 dB/(cm MHz^2) [8]. It is clear that the influence of attenuation in water is negligible in the investigated ranges of distances and given frequency band. The range of distances 0,30…3,00 mm was chosen to illustrate the distortion of waveforms' to be discussed in the field modelling part of present paper.

After acquisition into computer memory, the digitised signals were analysed in a MATLAB environment. The echo-pulses in the case of distilled water did not differ in between the distance changes. It should be mentioned that all half-periods in echo-pulses in case of water had a constant time duration of 32±1 ns within pulse length. Here 1 ns is a time sampling period. Such an averaged experimental waveform was used for excitation of models and is presented in Fig.4.

Digitally triggered echo-pulses what were acquired through castor oil are shown in the upper part of Fig.3. The triggering moment was chosen to be the moment in waveform of the first negative–to positive zero-crossing that is located near 100 ns in the time diagram.

The analysis shows that echo-pulses obtained through castor oil changes their half-period duration. The duration increases with distance or thickness of medium layer. As can be seen from the lower panel of Fig.3, the spectral maximum of the signal shifts down from 13,9 MHz at minimal distances up to 12,8 MHz at maximum distances. That is the characteristic feature of pulse spectra modification in lossy media [10].

Simulation results: plane wave attenuation

In plane wave case simulations, the same wave path length as in the experiments has been used. The echo-pulse experimentally acquired through distilled water as the primary waveform or excitation *v(t)* for the minimum-phase and time-causal models was used (Fig.4). Acoustic parameters of castor oil in both models: attenuation coefficient α_0=0,7 dB/(cm MHz^{1,67}) [7], and phase velocity at f_0=15 MHz, c_0=1511 m/s [7].

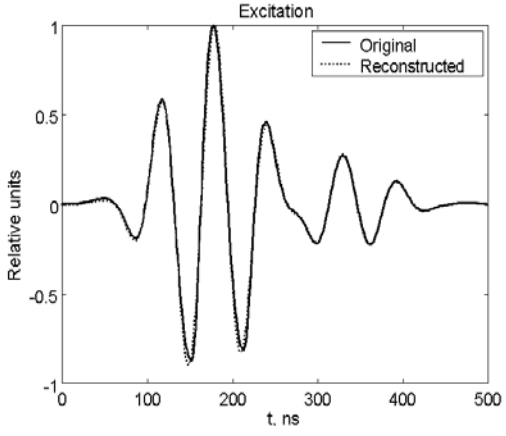

Fig.4. **Waveforms *(v(t))* used in the modelling distortions caused by attenuation and velocity dispersion in castor oil.**

The simulation procedure was as follows: the minimum-phase model expressed in equations (9) (10) and (11) was applied, while the spectrum decomposition time-causal model described in equation (5) and presented in Fig.1 was used also.

To apply the time-causal model, the excitation (Fig.4.) having a frequency band 5…25 MHz at the magnitude level –40 dB in accordance with [5] is decomposed into M=21 Gaussian band-limited pulses 1 MHz in bandwidth each. The reconstructed pulse is also drawn in the same diagram to show what error occurs after reconstruction.

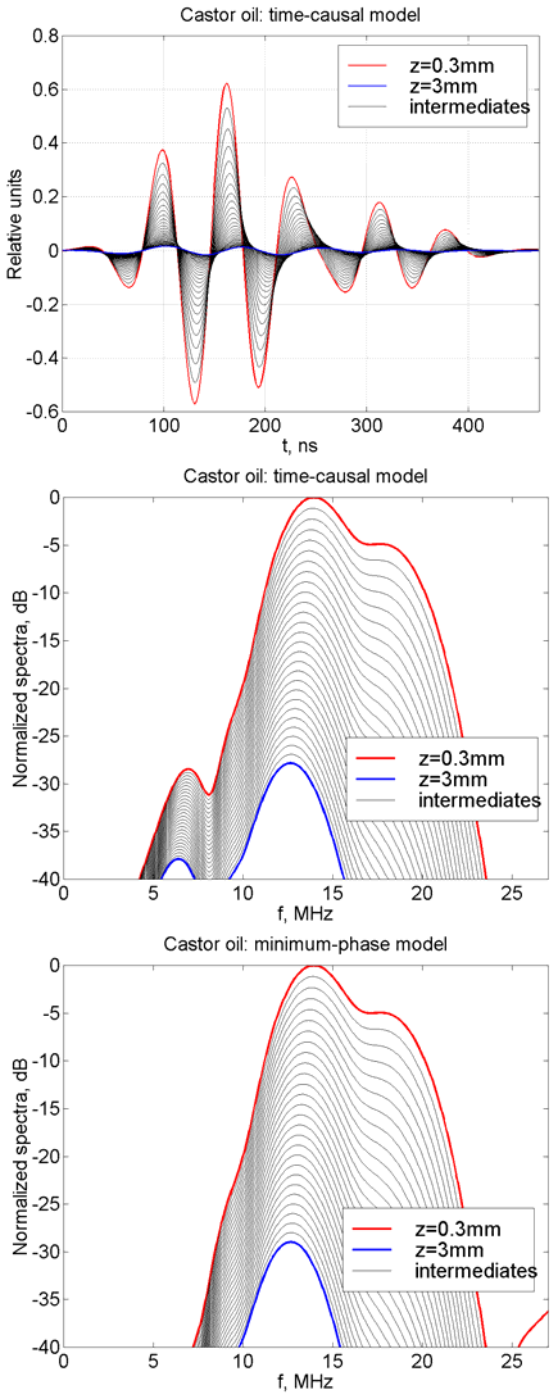

Fig.5. **Results of the simulation: the waveforms *(s(t))* of echo-pulses after simulated travelling through the different path lengths in castor oil. The spectra of echo-pulses obtained using minimum-phase and time-causal models**.

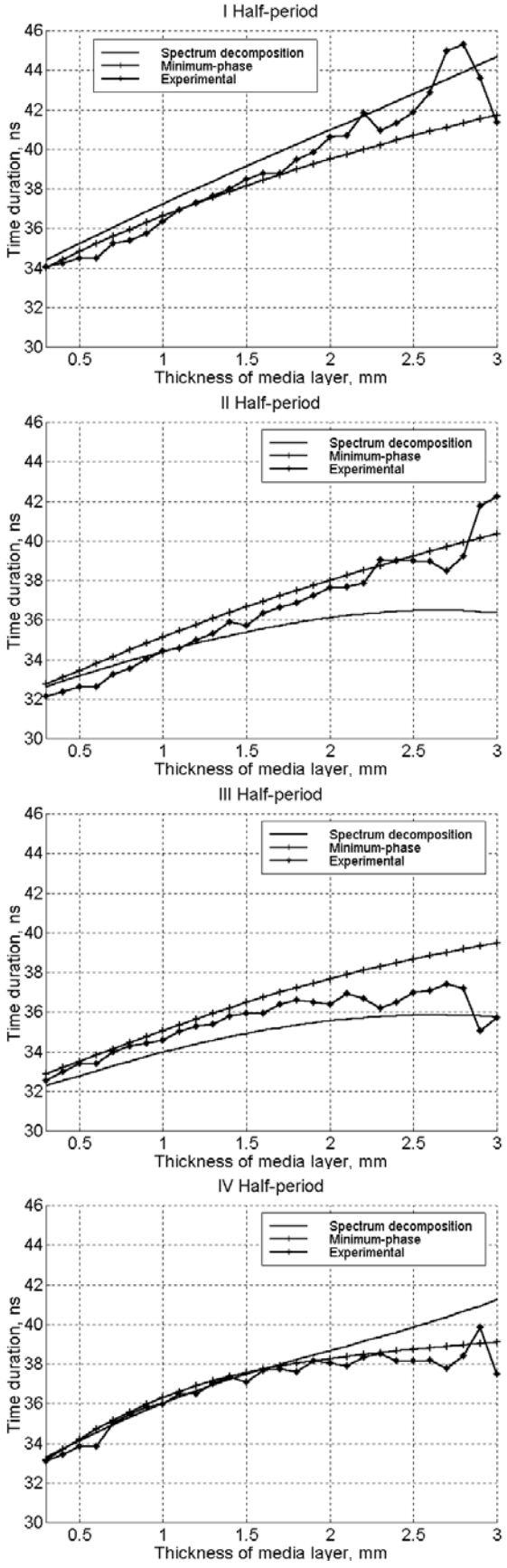

Fig.6. **A comparison of experimental echo-pulses with results obtained in minimum-phase and time-causal models: the change of half-period time duration caused by a change of castor oil layer thickness**.

The specific features in the calculation of Hilbert transform are involved because the acoustic system under simulation is not frequency band-limited in general. The problem of what criteria to use in choosing the cut-off frequency appears. Also the features of discrete time signal processing are involved as well; effects of time-domain aliasing and frequency-domain aliasing appear [4]. The basic rules followed in obtaining the presented results are: retaining the unchanged sampling frequency and number of samples in the signal as was used in the experimental investigation and in the time-causal model. Of course, we tried to avoid errors by verifying the impulse response intermediately during simulations and to eliminate any aliasing effects. In the discrete time domain the waveform length was 2048 with sampling period of 1 ns. Therefore folding frequency of 500 MHz was used as a cut-off frequency for discrete Hilbert transform. Such a set of sampling parameters allows one to get results comparable to time-causal model results.

The results of the simulation are presented in Fig.5. Because in the minimum-phase and time-causal models, simulated waveforms differ negligibly, only the time-causal model result is shown.

To analyse the modification in waveform of echo-pulses, the half-period time duration in experimental, minimum-phase and time-causal waveform models is investigated precisely (Fig.6). The four half-periods of waveforms in the time interval between 75…225 ns are taken into account. The zero-crossing instants were calculated using linear interpolation. The duration increases within 32…42 ns when the distance is increased from 0,30 to 3,00 mm.

The specific feature of minimum-phase model has been observed: the simulated reactions are right-time shifted. Such a difference in velocity obtained in minimum-phase and time causal model is discussed in discussion section.

Simulation results: Attenuation in transient field

On the basis of one-dimensional model of plane wave propagation in lossy media the three-dimensional problem of waves radiation by finite aperture is analysed herein. The round aperture of 7,5 mm in radius radiating the theoretical Gaussian pulse *v(t)* shown in Fig.7 is used for simulation. As usually in field simulations the signal of velocity of vibrations on aperture is used as the input variable. Ultrasonic field in this paper is characterised using the acoustic pressure distribution in media under investigation. So, acoustic reactions in the transient field points located at 7,5 mm from aperture are described using pressure waveform.

To expose clearly the influence of attenuation and dispersion on the space-distributed pulse the wave fronts of transient wave are represented in Fig.9 and 10. The zero-crossing time instants are considered as the wave front of transient wave. For clarity in diagrams of wave fronts, the fronts are plotted only within the regions of ultrasonic field where energy of the pulse wave is concentrated. The zero-crossing line is plotted in the front of transient waveform having amplitude envelope higher than 10 % of the maximum peak in the region under investigation. Peak

amplitudes have been normalised separately for each attenuation case.

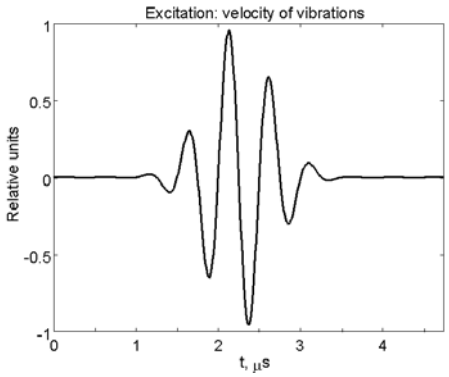

Fig.7. **Waveform of vibrations velocity *v(t)* for uniform excitation of aperture**.

The two approaches in modelling of modification of waves in lossy media are compered. The simplified one, when is considered that elementary waves contributing to particular space point travels the path of the constant length. Such a precondition could be satisfied in far field when acoustic path lengths for contributing waves are almost the same. The results of modelling for such conditions are presented in [2]. The mentioned preconditions are not satisfied in near field, where the exact solution must be applied. So, the one-dimensional (1D) approach in three-dimensional field modelling could be explained very simply by excluding sum 0…*N*-1 in the expression (6) or (7). This means, that in each discrete time instant the waves contributing to the field point has been travelling the path of length $R_{mean} = z + mean \cdot c_0 \tau$ instead of changing length $R_n = z + n \cdot c_0 \tau$ as it was written in (5) and (9). The *'mean'* is the index of path, which is arithmetic average of the minimum and maximum values: $R_{mean} = (R_{\max} + R_{\min})/2$ (see Fig.8.).

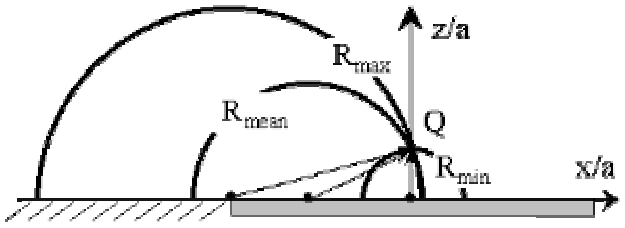

Fig.8. **The differences in acoustic path to travel for elementary spherical waves contributing to the point Q in different instants of discrete time $n\tau$.**

The waveforms drawn in Fig.3 or Fig.5 could be used to illustrate a 3D attenuation effect on contributions coming from elementary wave sources on the aperture (Fig.8). Such a modification of waveforms contributing to space point Q on the beam axis (z=R_{min}=0,6 mm, x=0) is possible when the round aperture of the radius $a = \sqrt{R_{\max}{}^2 - R_{\min}{}^2}$ uniformly radiates into the castor oil the pulse shown in Fig.4. So, in the case of R_{min}=0,6 mm, R_{max}=6 mm, the aperture radius must be a=5,9 mm.

Well, the non-simplified three-dimensional (3D) and simplified one-dimensional (1D) approaches in modelling of modification of travelling wave are used and the results compered in Fig.9 and Fig.10. In both figures the *y*-axis is the normalised distance from beam axis (called *x/a*) here aperture radius a=7,5 mm. The thickness of layer was z=7,5 mm. For the same input data the calculations in time-causal and minimum-phase models are done. The minimum-phase model has the cut-off frequency of 114 MHz, the sampling period of (9/1024) μs and number of samples of 1024 in waveform.

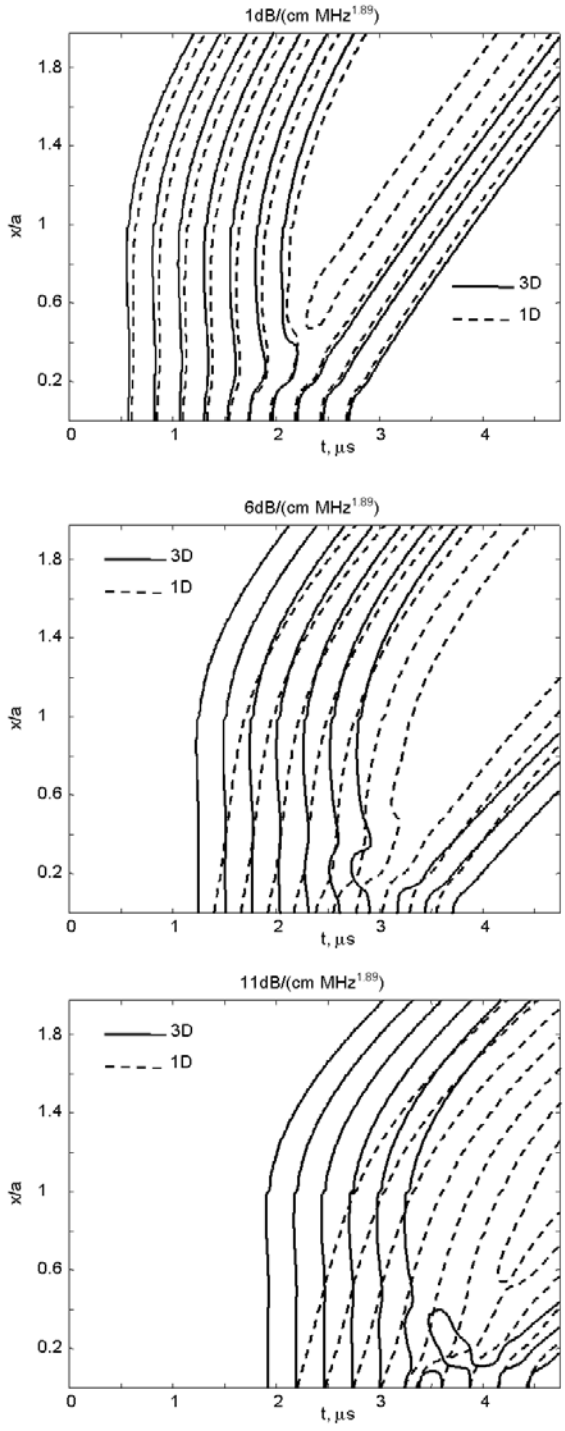

Fig.9**. Wave-fronts of three-dimensional pulse: Minimum-phase model, the 1*D* and 3*D* approaches compered in cases of different attenuation coefficients α_0 1; 6 and 11 dB/(cm MHz^{1,89}).**

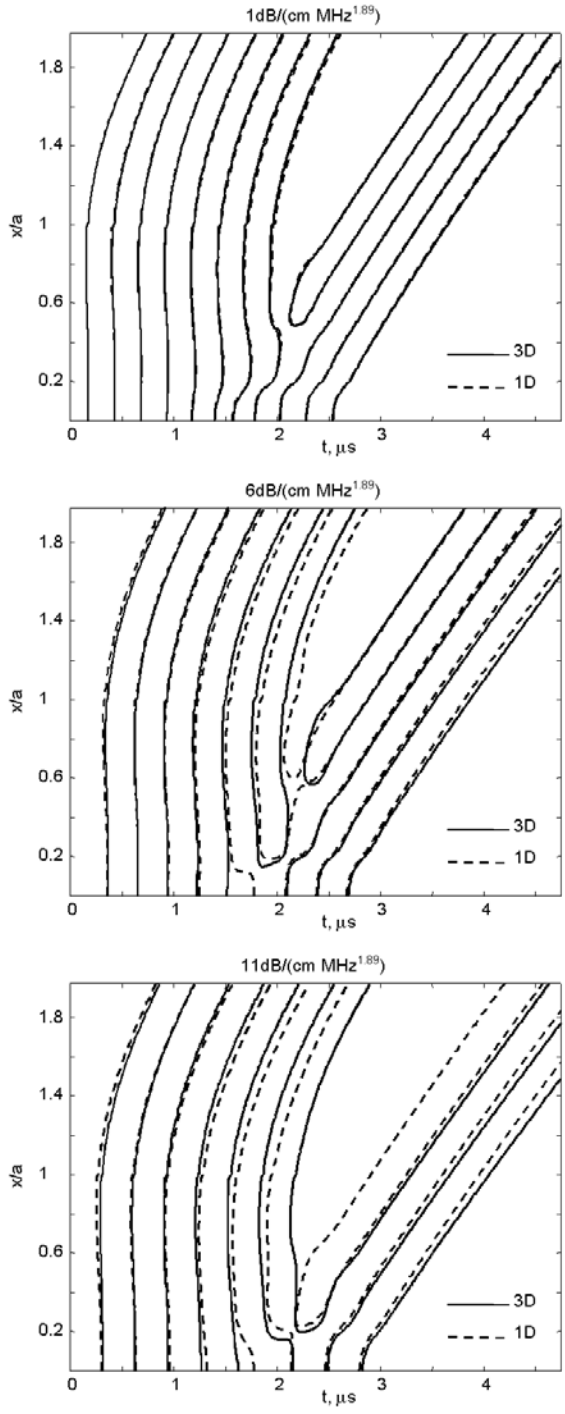

Fig.10. **Wave-fronts of three-dimensional pulse: Time causal model, the 1D and 3D approaches compered in cases of different attenuation coefficients 1, 6 and 11 dB/(cm MHz$^{1.89}$).**

The particular waveforms excluded from three-dimensional pulse wave has been normalised according to the amplitude of the waveform corresponding for the first case of attenuation (1 dB/(cm MHz^{1,89}), so the amplitude loss can be compared of the waveforms in Fig.11 and 12. Reaction waveform of acoustic pressure within the beam axis (x/a=0) at the distance z/a=1 from aperture is plotted in the upper panels of Fig.11 and 12. The lower panels shows the waveforms of reaction at x/a=1, z/a=1. In Fig.12 the right-time shift of waveforms is present. Such a time delay has no physical background. That is only the specific feature of minimum-phase model.

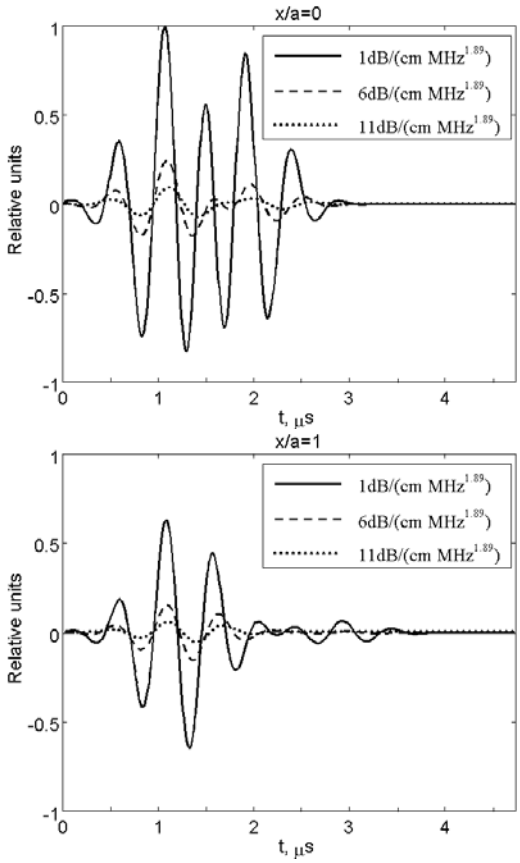

Fig.11. **Reaction waveforms at space points (*x/a*=0, *z/a*=1*) and (x/a*=1, *z/a*=1*)* each corresponding to different attenuation: Time-causal model, 3D approach.**

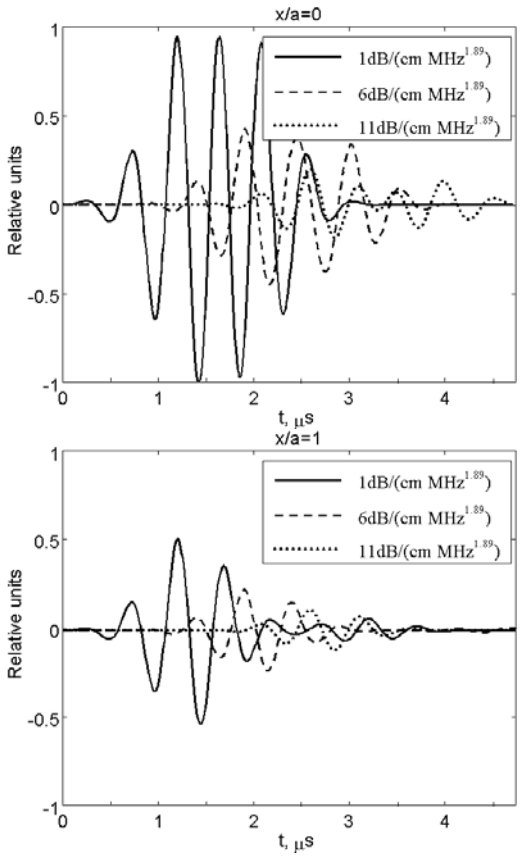

Fig.12. **Reaction waveforms at space points (*x/a*=0, *z/a*=1*) and (x/a*=1, *z/a*=1*)* each corresponding to different attenuation: Minimum-phase model, 3D approach**.

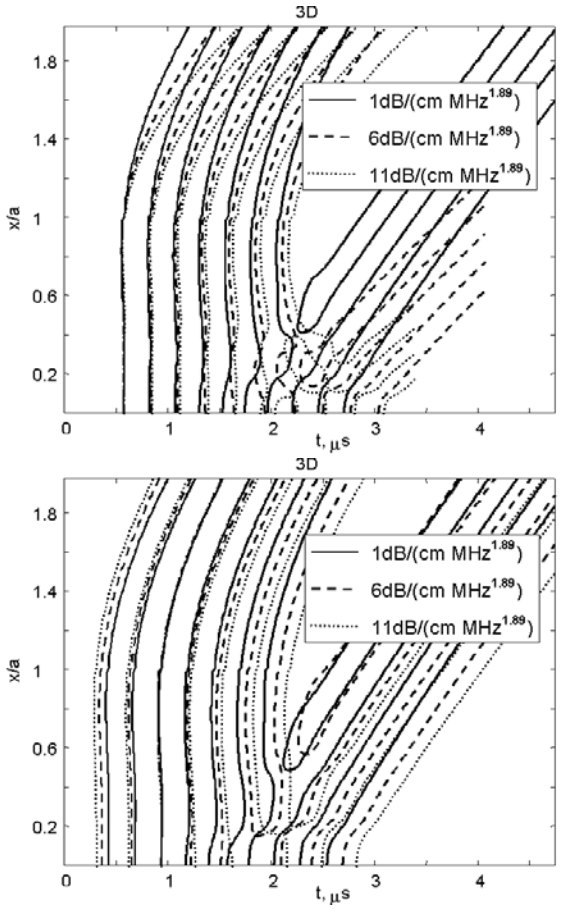

Fig.13. **Comparison of wave fronts attained in cases of attenuation coefficients 1, 6 and 11 dB / (cm MHz$^{1.89}$): upper panel – minimum-phase model; lower panel – time-causal model.**

All the waveforms in one diagram are calculated at the same distance *(z/a=1)* from aperture, only the attenuation coefficients are different for each of them. Regardless of minimum-phase model insensibility to the attenuation and travelling the wave fronts are left-shifted and compered in upper panel of Fig.13. So, diagrams of wave-fronts in upper panel of Fig.13 are manually aligned for first zero-crossing. The alignment of diagrams of wave-fronts obtained from time-causal model are not changed manually to expose the earlier arrival in case of more attenuating media.

Simulation results: Attenuation in stationary field

Theoretical and experimental harmonic excitation fields in lossless medium are presented in Fig.16. The acoustic pressure amplitude distribution is visualised using gray-scale: the lighter the higher the amplitude. The lateral and longitudinal distances are normalised according to the aperture radius, what was a=3,2 mm. The measurements are done in water (lossless media, α_0=0,0022 dB/(cm MHz^2) using hydrophone of 0,2 mm in diameter [11]. All the simulation results were obtained from the minimum-phase model using 3D approach. Calculation parameters were as follows: the cut-off frequency for discrete Hilbert transform was 171 MHz, the sampling period was (6/2048) μs with number of samples of 2048 in waveform.

Most noticeable difference in pressure distributions is the loss of amplitude in far field when the attenuation coefficient is increased. There must be pointed that such a difference in near regions of calculated and measured fields is caused by non-uniform radiation of the real aperture what has been not taken into account during modelling.

To expose the specifics in amplitude distribution of stationary field when modification of contributing waves is performed in 1D and 3D approaches the difference diagrams are show in Fig.14 and 15. That diagrams use the same pressure amplitude data as the third and forth amplitude distribution in Fig.16, but the modelling of attenuation influence is different: 1D and 3D. The pressure amplitude for each case of attenuation was normalized according to the pick amplitude in lossless media then the differences of normalized amplitudes are calculated and drawn in Fig. 14 and 15.

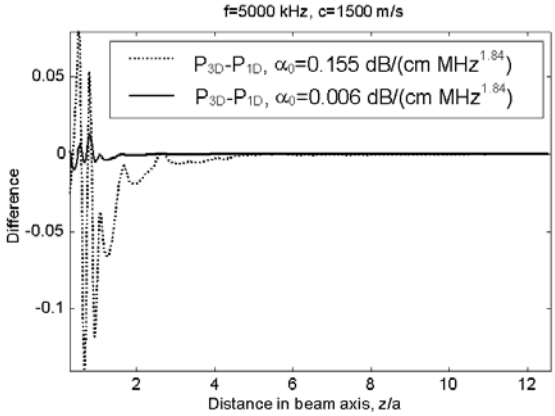

Fig.14. **Normalized differences of pressure amplitude on the axis of ultrasonic beam: because of the 3D and 1D simulation of attenuation influence in minimum-phase model.**

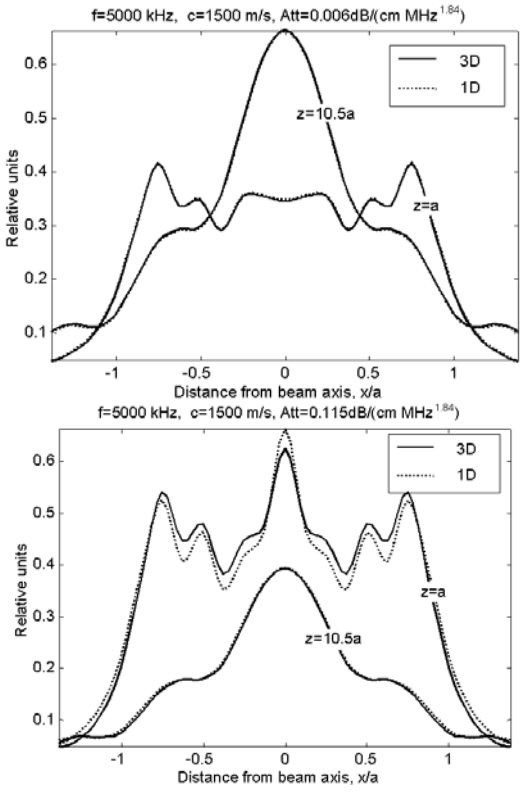

Fig.15**. Normalized amplitude of pressure in cross-sections (*z*=10.5*a* ans *z*=*a*) of ultrasonic beam caused by 3D and 1D simulation of attenuation influence in minimum-phase model, attenuation coefficients 0.006 and 0.115 dB/(cm MHz$^{1.84}$)**

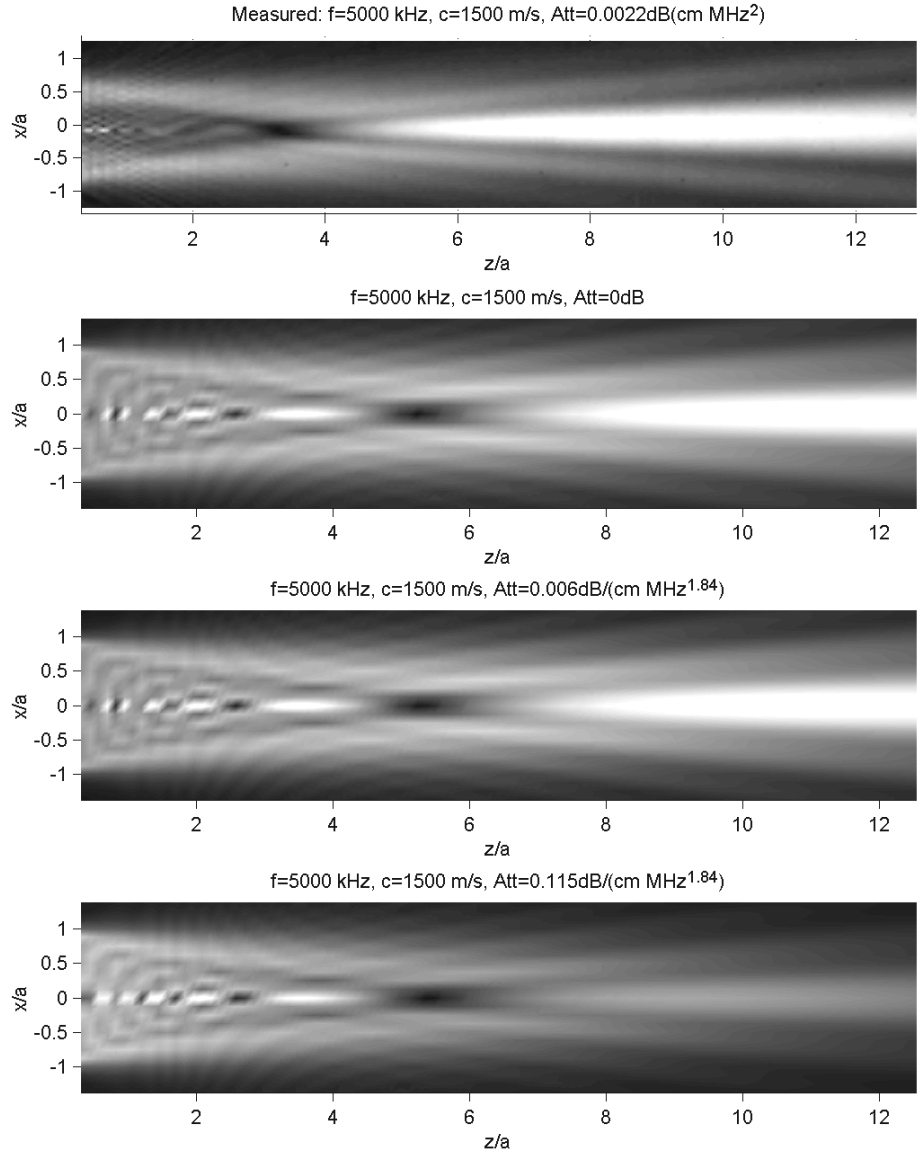

Fig.16. **Distribution of pressure amplitude in stationary ultrasonic field: upper panel – measured field in weakly attenuating medium, the rest – minimum-phase simulation results for different attenuation: 0, 0.006 and 0.115 dB/(cm MHz$^{1.84}$)**

The result obtained from 1D and 3D differ according to the product of the difference in the distances what contributing waves were covered (R_{max}-R_{min}) and of the attenuation coefficient α_0. The higher the product value the higher the difference.

Discussions

The results obtained in the experiment with castor oil have showed that the effect of ultrasound attenuation and speed dispersion on the distortion of waveform is possible to simulate accurately using either the minimum-phase or the time-causal model. The value of power y in frequency functions of attenuation greater that *1* is not the reason for the minimum-phase model to fail. An incorrect result is possible if the attention for the time-domain or frequency-domain aliasing effects is not taken.

It must be pointed out that only the distortion of pulse shape or spectra of the pulse has been investigated not taking into account absolute delay of the pulse. The minimum-phase model takes into account the product αR, therefore is impossible to separate whether such attenuation is gained because of the long path-length in weakly attenuating medium, or because of the short path-length in the highly attenuating medium. It was thought that the absolute time delay is the weak part of the minimum-phase model, because the model does not separate the attenuation from the propagation. But the analysis of the phase response $\beta(f,R)$ resulting from discrete Hilbert transform (11) gives that set of responses calculated for set of thickness (R=0,6…6,0 mm) is spaced with the step proportional with to the step in R. Actually the phase velocity $c_p(\omega)$ is related to the phase response by relation: $c_p(\omega)=(\omega R)/\beta(\omega,R)$. After such a scaling of the set of phase responses $\beta(\omega,R)$ we get the single relative dispersion function of phase velocity of wave propagation in castor oil. In time-causal model predicted dispersion could be calculated from (3) and (4) as fallow: $c_p(\omega)=(\omega R)/(\varphi+\omega T)$ [5]. So, the dispersion functions normalised according to the velocity c_0 for central frequency what were used both in minimum-phase and in time causal model are compared in Fig.17.

This deficiency of the minimum-phase model clearly appears in the wave-front diagrams in Fig.9, also in the response waveforms shown in Fig.12. The reason of differences in waveforms of responses in the same space points but obtained using minimum-phase model and time-causal model (Fig.11 and 12) must be also refereed as lack of minimum-phase model.

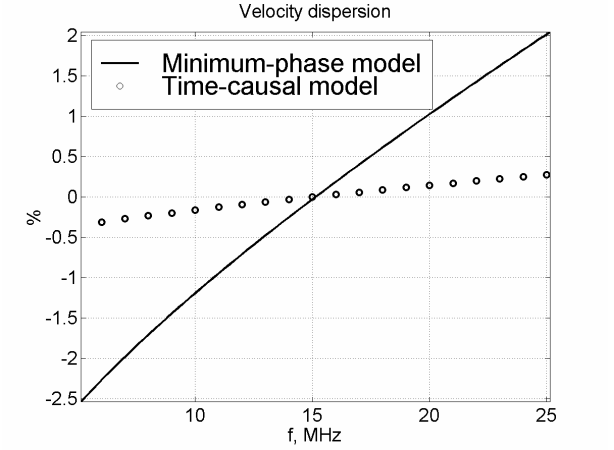

Fig.17. **Comparison of velocity dispersions in castor oil: predicted from time-causal model (circles), and predicted from discrete Hilbert transform (11) (solid line).**

On the basis of such results it could be pointed out, that from the strict point of view, the minimum-phase model reproduces a continuos changing velocity of wave propagation, while time-causal model uses the finite number of constant velocities, predicted for each narrowband component (our case M=21). The time delay of pulses calculated from minimum-phase model has no physical background therefore the wave-fronts calculated using time-causal model could be considered as more reliable.

Although time-causal model is evaluated to give the causal response we get an earlier arrival with increased attenuation. The causes of such a model performance are not clear up to now. The same result is published by Wismer et.al. [12], where the wave equation with complex wavenumber was calculated. Besides, the dispersion in complex wavenumber has been introduced accordingly to the time-causal theory from [6].

The results presented therein are to be discussed in the logical way. The stated model taking into account wave diffraction from finite aperture together with wave attenuation and speed dispersion could be in part tested analysing the given results when the 1D and 3D approaches of attenuation influence are applied. The specific effect of 3D approach is clearly depicted in Fig.14: the pressure amplitude is overestimated in the near field when 1D approach is applied.

It could be asserted that 3D attenuation influence approach does the expected.

Achnowledgement

R. Jurkonis is thankful to colleagues V.Petkus (KTU, Telematics Scientific Lab.) and T.Jansson (Lund University, Electrical Measurements Dept.) for expressed enthusiasm and collaboration.

References

1. **Berkhoff A. P., Thijssen J. M. and Homan R. J. F.** Simulation of ultrasonic imaging with linear arrays in causal absorptive media //Ultrasound in Med. & Biol., Vol.22. No.2. 1996. P.245-259,
2. **Jensen J. A., Gandhi D. and O'Brien W. D.** Ultrasound fields in an attenuating medium. //IEEE Ultrasonic Symposium Proceedings. Vol.2. 1993. P.943-946.
3. **Lukoševičius A. and Jurkonis R.** Ultragarsinio artimojo lauko charakteristikų slopinančioje aplinkoje apskaičiavimo metodas. //Ultragarsas. Nr.2(27). 1997. P.33-37.
4. **Kuc R.** Modelling acoustic attenuation of soft tissue with minimum-phase filter.// Ultrasonic Imaging. Vol.6. 1984. P.24-36.
5. **He P.** Simulation of ultrasound pulse propagation in lossy media obeying a frequency power law.// IEEE Transactions on Ultrasonic, Ferroelectrics and Frequency Control. Vol.45. No.11998.. P.114-125.
6. **Szabo T. L.** Causal theories and data for acoustic attenuation obeying a frequency power law.// J. Acoust Soc. Am. Vol.97(1). 1995. P.14-24.
7. **He P.** Experimental verification of models for determining dispersion from attenuation.// IEEE Transactions on Ultrasonic, Ferroelectrics and Frequency Control. Vol.46. No.3. 1999. P.706-714.
8. **Kino G.** Acoustic waves: devices, imaging and analog signal processing. // Englewood Cliffs, New Jersey: Prentice-Hall, 1987.
9. **Poularikas A. D.** The Transforms and Applications Handbook: Second Edition. - Boca Raton: CRC Press LLC, 2000.
10. **Ophir J. and Jaeger P.** Spectral shift of ultrasonic propagation through media with nonlinear dispersive attenuation.// Ultrasonic Imaging. Vol.4. 1982. P.282-289.
11. **Jansson T., Jurkonis R., Mast T. D., Persson H. W. and Lindstrom K.** Frequency dependence of speckle in continuous-wave ultrasound: implications for blood perfusion measurements.// IEEE Transactions on Ultrasonic, Ferroelectrics and Frequency Control. (submitted 17 November, 1999).
12. **Wismer M. G. and Ludwig R.** An Explicit Numerical Time Domain Formulation to Simulate Pulsed Pressure Waves in Viscous Fluids Exhibiting Arbitrary Frequency Power Law Attenuation. // IEEE Transactions on Ultrasonic, Ferroelectrics and Frequency Control. Vol.42. No.6. 1995. P.1040-1049.

R.Jurkonis, A.Lukoševičius

Ultragarsinis laukas slopinančioje aplinkoje: kai kurie modeliavimo ir eksperimentų rezultatai

Reziumė

Straipsnyje ultragarso slopinimas aplinkoje modeliuojamas panaudojant spektrinės dekompozicijos bei minimalios fazės filtro metodus, siekiant išlaikyti modeliuose priežastingumo principą. Modeliuojant ultragarsinį impulsinį ir harmoninį signalinius laukus, generuojamus ultragarsinio keitiklio slopinančioje aplinkoje, panaudotas naujas algoritmas, įvertinantis artimo lauko efektus. Pateikti ultragarsinių signalų sklidimo eksperimentinio tyrimo rezultatai, laukų matavimai. Parodyta, kad slopinimas turi didelę įtaką laikiniam ir spektriniam ultragarsiniuose matavimuose naudojamų signalų, pasiskirstymui erdvėje, todėl į jį reikėtų atsižvelgti analizuojant matavimų rezultatus.

Pateikta spaudai: 2000 05 23

DOI: 10.5755/j01.u.35.2.7968